

RISnet: A Scalable Approach for Reconfigurable Intelligent Surface Optimization with Partial CSI

Bile Peng*, Karl-Ludwig Besser†, Ramprasad Raghunath*, Vahid Jamali‡, Eduard A. Jorswieck*

*Institute for Communications Technology, Technische Universität Braunschweig, Germany

†Department of Electrical and Computer Engineering, Princeton University, USA

‡Department of Electrical Engineering and Information Technology, Technische Universität Darmstadt, Germany

Email: {b.peng, r.raghunath, e.jorswieck}@tu-braunschweig.de, karl.besser@princeton.edu, vahid.jamali@tu-darmstadt.de

Abstract—The reconfigurable intelligent surface (RIS) is a promising technology that enables wireless communication systems to achieve improved performance by intelligently manipulating wireless channels. In this paper, we consider the sum-rate maximization problem in a downlink multi-user multi-input-single-output (MISO) channel via space-division multiple access (SDMA). Two major challenges of this problem are the high dimensionality due to the large number of RIS elements and the difficulty to obtain the full channel state information (CSI), which is assumed known in many algorithms proposed in the literature. Instead, we propose a hybrid machine learning approach using the weighted minimum mean squared error (WMMSE) precoder at the base station (BS) and a dedicated neural network (NN) architecture, RISnet, for RIS configuration. The RISnet has a good scalability to optimize 1296 RIS elements and requires partial CSI of only 16 RIS elements as input. We show it achieves a high performance with low requirement for channel estimation for geometric channel models obtained with ray-tracing simulation. The unsupervised learning lets the RISnet find an optimized RIS configuration by itself. Numerical results show that a trained model configures the RIS with low computational effort, considerably outperforms the baselines, and can work with discrete phase shifts.

Index Terms—Reconfigurable intelligent surfaces, space-division multiple access, unsupervised machine learning, partial channel state information, ray-tracing channel model.

I. INTRODUCTION

The reconfigurable intelligent surface (RIS) is a promising technology that has been attracting increasing attention in recent years. An RIS is a planar array of many passive, reconfigurable elements that can reflect incoming electromagnetic waves with shifted complex phases [1]. As an important application of the RIS, we consider the sum-rate maximization problem in a downlink RIS-assisted multi-user multi-input-single-output (MISO) channel with space-division multiple access (SDMA), which is a joint optimization problem of precoding at the base station (BS) and the RIS configuration. In the literature, the weighted minimum mean squared error (WMMSE) precoder [2] is proposed as an optimal precoder

for weighted sum-rate maximization with SDMA. On the RIS side, many different approaches for optimizing the RIS configuration have been presented in previous works. This includes block coordinate descent (BCD) to maximize the weighted sum-rate [3], majorization-maximization and the efficient alternating direction method of multipliers (ADMM) to optimize the sum-rate [4], [5] and the sum-rate of multiple user groups [6]. Riemannian manifold conjugate gradient (RMCG) and the Lagrangian method are applied to optimize multiple RISs and BSs to serve users on the cell edge [7]. Exhaustive search and successive refinement algorithm are applied to improve passive beamforming [8]. The configuration of active RISs is optimized with the successive convex approximation algorithm to maximize the signal-to-noise ratio in [9]. Gradient-based optimization is applied to maximize the effective rank and the minimum singular value [10].

These analytical iterative methods do not scale well with the number of RIS elements in general. No more than 100 RIS elements are assumed in [3]–[9] and up to 400 RIS elements are assumed in [10], which is still far from the vision of more than 1000 RIS elements [1]. In fact, it has been shown that for most typical scenarios, large RISs with several hundreds to several thousands of elements are needed in order to establish a sufficient link budget [11].

Moreover, it is common that suboptimal approximations (e.g., [3], [8]) have to be made for these approaches, which degrade the performance. On the other hand, machine learning models require much computational resources in training but the trained model can perform inference almost instantly. They are more flexible due to the universal approximation theorem [12] such that they do not have to make suboptimal approximations. If the model is trained properly on a representative training set, the machine learning approach can achieve a better performance. In recent years, deep learning [13]–[15], deep reinforcement learning [16] and meta learning [17] have been applied to optimize the RIS. However, scalability is still an open problem because the model complexity grows with the number of RIS elements. Therefore, existing works employing machine learning only assume a limited number of RIS elements (no more than 100 in [14]–[17] and 256 in [13]).

Another common disadvantage of many references on RIS-assisted communication systems is the full channel state information (CSI) assumption (e.g., [3], [5], [6], [8], [9],

The work is supported in part by the Federal Ministry of Education and Research Germany (BMBF) as part of the 6G Research and Innovation Cluster 6G-RIC under Grant 16KISK031. The work of K.-L. Besser is supported by the German Research Foundation (DFG) under grant BE 8098/1-1. The work of V. Jamali is supported in part by the German Research Foundation (DFG) as part of project C8 within the Collaborative Research Center (CRC) 1053-MAKI and in part by the LOEWE initiative (Hesse, Germany) within the emergenCITY center.

[15]). Due to the large number of RIS elements, the full CSI of all elements is extremely difficult to obtain in real time. Possible countermeasures are, e.g., codebook-based RIS optimization [11], [18]. However, the beam training is still a bottleneck.

To address the above issues, we introduce a neural network (NN) architecture *RISnet*, which was first proposed in [19] and receives significant improvements in this work, including the arbitrary number of users with permutation-invariance, partial CSI, and validation with more realistic ray-tracing channel models. The proposed approach has the following two advantages:

- 1) We use the same filters to all RIS elements and users. The number of parameters in the NN is therefore independent from the number of RIS elements, which improves the scalability significantly. We demonstrate this by applying *RISnet* to a scenario with 4 users and 1296 RIS elements in Section IV.
- 2) *RISnet* supports partial CSI as input, which reduces the difficulty of channel estimation considerably (phase shifts of 1296 RIS elements are computed based on the CSI of 16 RIS elements).

Furthermore, we show that our proposed approach computes the precoding matrix and RIS phase shifts in milliseconds, outperforms the baselines significantly, and works with discrete phase shifts, which is a more realistic assumption compared to continuous phase shifts for e.g., PIN-diode based RIS elements..

II. SYSTEM MODEL AND PROBLEM FORMULATION

We consider a downlink RIS aided communication from a multi-antenna BS to multiple users, as shown in Figure 1. The channel from BS to RIS is denoted as $\mathbf{H} \in \mathbb{C}^{N \times M}$, where N is the number of RIS elements and M is the number of BS antennas. The channel from RIS to users is denoted as $\mathbf{G} \in \mathbb{C}^{U \times N}$, where U is the number of users. The channel from BS directly to users is denoted as $\mathbf{D} \in \mathbb{C}^{U \times M}$.

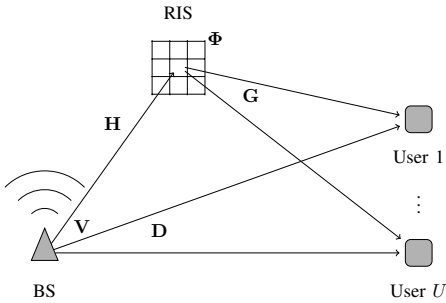


Figure 1. System model.

The objective is to use SDMA to maximize the sum-rate of the users. The BS can perform precoding subject to maximum transmit power constraint E_{Tr} . Each RIS element can receive the signal from the BS, shift the complex phase of the signal, and reflect signal without changing its amplitude.

We denote the precoding matrix as $\mathbf{V} \in \mathbb{C}^{M \times U}$. The diagonal matrix $\Phi \in \mathbb{C}^{N \times N}$ is the signal processing matrix at the RIS. The diagonal element in row n and column n is $\phi_{nn} = e^{j\psi_n}$, where $\psi_n \in [0, 2\pi)$ is the phase shift of RIS element n . The signal received at the users is given as

$$\mathbf{y} = (\mathbf{G}\Phi\mathbf{H} + \mathbf{D})\mathbf{V}\mathbf{x} + \mathbf{n}, \quad (1)$$

where $\mathbf{x} \in \mathbb{C}^{U \times 1}$ is the transmitted symbols, $\mathbf{y} \in \mathbb{C}^{U \times 1}$ is the received symbols and $\mathbf{n} \in \mathbb{C}^{U \times 1}$ is the thermal noise.

Let $\mathbf{C} \in \mathbb{C}^{U \times U}$ be the combined matrix of precoding and transmission, i.e.,

$$\mathbf{C} = (\mathbf{G}\Phi\mathbf{H} + \mathbf{D})\mathbf{V} \quad (2)$$

and c_{uv} be the element in row u and column v of \mathbf{C} . The problem to maximize the sum-rate subject to the maximum transmit power can be given by

$$\max_{\mathbf{V}, \Phi} L = \sum_{u=1}^U \log_2 \left(1 + \frac{|c_{uu}|^2}{\sum_{v \neq u} |c_{uv}|^2 + \sigma^2} \right) \quad (3a)$$

$$\text{s.t. } \text{tr}(\mathbf{V}\mathbf{V}^H) \leq E_{Tr} \quad (3b)$$

$$|\phi_{nn}| = 1 \quad (3c)$$

$$|\phi_{nn'}| = 0 \text{ for } n \neq n', \quad (3d)$$

where σ^2 is the noise power.

In this problem, we optimize both precoding \mathbf{V} at BS and RIS phase shifts Φ . While optimizing Φ is a new and open problem, the WMMSE precoder is proved to be the optimal precoder to maximize the weighted sum rate (WSR). It is shown that minimizing weighted mean squared error (MSE) is equivalent to maximizing WSR [2]. By iteratively updating precoding vectors and weights of MSE, the WSR is maximized. We choose the WMMSE precoder for the precoding in BS. It is to note that \mathbf{V} and Φ must be jointly optimized because their optimal values depend on each other. However, the iterative approach of WMMSE precoder makes it not differentiable and the gradient ascent cannot be applied to optimize the NN. To tackle this problem, we apply alternating optimization (AO), which updates \mathbf{V} and phase shift matrices Φ alternatively while keeping the other constant for all the data samples.

III. PROPOSED MACHINE LEARNING SOLUTION

The aim of solving problem (3) is to jointly optimize the precoding matrix \mathbf{V} and the phase adjustments of the RIS elements Φ . Since it is difficult to find an optimal solution to this problem due to its high dimensionality (the large number of RIS elements), we propose solving (3) by employing machine learning. In particular, we train an NN to learn the mapping between the available CSI, the optimal precoding and phase adjustments.

A. Framework of Unsupervised Machine Learning

We define a neural network N_θ parameterized by θ , which maps from the CSI to the RIS phase shifts Φ . Since N_θ cannot take the original CSI as input, we define channel feature Γ as an equivalent CSI presentation, as will be explained in

Section III-B. Hence, we have $\Phi = N_\theta(\Gamma)$. Applying the WMMSE precoder, the objective function L defined in (3) is fully determined by Γ and Φ . We can write the objective as $L(\Gamma, \Phi) = L(\Gamma, N_\theta(\Gamma); \theta)$. Note that we emphasize L depends on the parameter θ given Γ here. We collect massive channel features in a training set \mathcal{D} and formulate the unsupervised machine learning problem as

$$\max_{\theta} \sum_{\Gamma \in \mathcal{D}} L(\Gamma, N_\theta(\Gamma); \theta). \quad (4)$$

In this way, we optimize N_θ which maps from any $\Gamma \in \mathcal{D}$ to Φ . If the training set is general enough, we would expect that a channel feature $\Gamma' \notin \mathcal{D}$ can also be mapped to a good Φ .

B. Channel Feature

In the RIS-assisted channel, there are three channel matrices \mathbf{H} , \mathbf{G} and \mathbf{D} , among which \mathbf{H} is assumed to be constant because BS and RIS are stationary and the environment is relatively invariant, \mathbf{G} and \mathbf{D} depend on user positions and are inputs of N_θ . We would like to define a feature γ_{un} for user u and RIS element n such that we can apply the same filters to every user and RIS element to enable scalability. Since g_{un} in row u and column n of \mathbf{G} is the channel gain from RIS element n to user u , we can simply include amplitude and phase of g_{un} in γ_{un} ¹. On the other hand, elements in \mathbf{D} cannot be mapped to RIS elements because \mathbf{D} is the channel from BS directly to users. Therefore, we define $\mathbf{J} = \mathbf{D}\mathbf{H}^+$, where $(\cdot)^+$ denotes the pseudo-inverse operation, and (1) becomes $\mathbf{y} = (\mathbf{G}\Phi + \mathbf{J})\mathbf{H}\mathbf{V}\mathbf{x} + \mathbf{n}$, i.e., signal \mathbf{x} is precoded with \mathbf{V} , transmitted through channel \mathbf{H} to the RIS, and through channel $\mathbf{G}\Phi + \mathbf{J}$ to users. Elements j_{un} of \mathbf{J} is the channel gain from RIS element n to user u . The features of user u and RIS element n can then be defined as $\gamma_{un} = (|g_{un}|, \arg(g_{un}), |j_{un}|, \arg(j_{un}))^T \in \mathbb{R}^{4 \times 1}$, where $|a|$ and $\arg(a)$ are amplitude and phase of complex number a , respectively. The complete channel feature $\Gamma \in \mathbb{R}^{4 \times U \times N}$ is a three dimensional tensor, where elements with index u and n in second and third dimensions are γ_{un} .

C. RISnet Architecture with Full CSI

The RISnet comprises L layers. In each layer, we would like to apply the same filters to all users and RIS elements in order to realize scalability. However, the optimal phase shift of an RIS element depends on all users and all RIS elements. Therefore, in every layer of the NN, we apply four filters for information processing of current user and current RIS element (cc), current user and all RIS elements (ca), other users and current RIS element (oc), and other users and all RIS elements (oa). Denote the input feature of user u and RIS element n in

layer i as $\mathbf{f}_{un,i}$ (in particular, $\mathbf{f}_{un,1} = \gamma_{un}$), the output feature of user u and RIS element n in layer i is calculated as

$$\mathbf{f}_{un,i+1} = \begin{pmatrix} \text{ReLU}(\mathbf{W}_i^{cc}\mathbf{f}_{un,i} + \mathbf{b}_i^{cc}) \\ (\sum_{n'} \text{ReLU}(\mathbf{W}_i^{ca}\mathbf{f}_{un',i} + \mathbf{b}_i^{ca})) / N \\ (\sum_{u' \neq u} \text{ReLU}(\mathbf{W}_i^{oc}\mathbf{f}_{u'n,i} + \mathbf{b}_i^{oc})) / (U-1) \\ (\sum_{u' \neq u} \sum_{n'} \text{ReLU}(\mathbf{W}_i^{oa}\mathbf{f}_{u'n',i} + \mathbf{b}_i^{oa})) / (N(U-1)) \end{pmatrix} \quad (5)$$

for $i < L$, where $\mathbf{W}_i^{cc} \in \mathbb{R}^{Q_i \times P_i}$ is trainable weights of class cc in layer i with the input feature dimension P_i in layer i (i.e., $\mathbf{f}_{un,i} \in \mathbb{R}^{P_i \times 1}$) and output feature dimension Q_i in layer i of class cc, $\mathbf{b}_i^{cc} \in \mathbb{R}^{Q_i \times 1}$ is trainable bias of class cc in layer i . Similar definitions and same dimensions apply to classes ca, oc and oa. For class cc in layer i , the output feature of user u and RIS element n is computed by applying a conventional full-connected layer (a linear transform with weights \mathbf{W}_i^{cc} and bias \mathbf{b}_i^{cc} and the ReLU activation) to $\mathbf{f}_{un,i}$ (the first line of (5)). For class ca in layer i , we first apply the conventional linear transform with weights \mathbf{W}_i^{ca} and bias \mathbf{b}_i^{ca} and ReLU activation to $\mathbf{f}_{un,i}$, then compute the mean value of all RIS elements. Therefore, the output feature of class ca for user u and all RIS elements is the same (the second line of (5)). For classes oc and oa, the information processing is similar but the output feature of user u is not computed with the input feature of user u , but is averaged over results of users other than user u (the third and fourth lines of (5)). We can infer from the above description that $\mathbf{f}_{un,i+1} \in \mathbb{R}^{4Q_i \times 1}$ for all u and n because the output feature comprises of four classes. Therefore $P_{i+1} = 4Q_i$. The whole output feature $\mathbf{F}_{i+1} \in \mathbb{R}^{4Q_i \times U \times N}$ is a three dimensional tensor, where elements with index u and n in second and third dimensions are $\mathbf{f}_{un,i+1}$. We see from (5) that all four parts of $\mathbf{f}_{un,i+1}$ use \mathbf{F}_i to compute the output features. The output feature of the current user and RIS element depends exclusively on the current user and RIS element (class cc, i.e., first part of $\mathbf{f}_{un,i+1}$) and the output feature of the other users and/or all RIS elements is the mean of the raw output of other users and/or all RIS elements (other classes, i.e., second to fourth parts of $\mathbf{f}_{un,i+1}$). Therefore, it should contain sufficient local and global information to make a wise decision on ψ_n . For the final layer, we use one filter to process the information. Features of different users are summed up to be the phase shifts because all the users share the same phase shift. Because the information processing before the final layer is symmetric to users and addition in the final layer is commutative, the RISnet is permutation-invariant to users, i.e., if we permute the users in the input, the output of RIS phase shifts does not change. This is a desired property that can enhance the generality of the NN. The information processing of a layer is illustrated in Figure 2.

In this way, we achieve a good scalability with the RISnet. However, it is difficult to obtain the full CSI (γ_{un} for every user and RIS element) in practice. Therefore, we propose to use partial CSI as input to RISnet.

¹The NN does not take complex numbers as input.

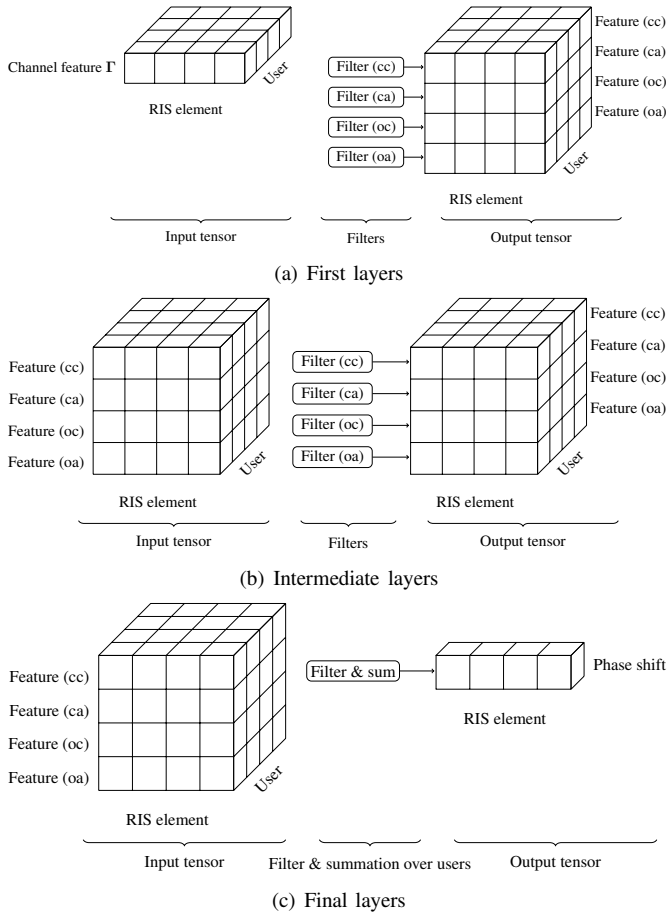


Figure 2. Information processing of layers in RISnet.

D. RISnet Architecture with Partial CSI

In this section, we assume an RIS architecture where only a few RIS elements are equipped with RF chains for channel estimation. Only a partial CSI can be estimated with pilot signals from the users by these RIS elements. If the propagation paths in the channel are mostly specular or line-of-sight (LoS) paths that contribute to channel gains of all RIS elements, the full CSI can be inferred from partial CSI because all RIS elements share the same propagation paths (with different path loss and complex phase). This fact suggests that we can use partial CSI as input to RISnet and compute phase shifts for all RIS elements. Rather than performing an explicit full CSI prediction like an image super-resolution, we perform an implicit full CSI prediction, i.e., an end-to-end learning from partial CSI to full RIS configuration.

The input channel feature for the RISnet with partial CSI in this section is channel features of all users and RIS elements with the ability to estimate the CSI. In the first layer, only these RIS elements are taken into consideration. Define an RIS element which has been taken into consideration of the RISnet as an *anchor element*, and a layer in RISnet that expands the anchor elements as an *expansion layer*, the RISnet expands the anchor elements from the RIS elements with CSI to all RIS elements. The basic idea of the expansion layer is to apply the

same filter to an adjacent RIS element with the same relative position to the anchor element, as shown in Figure 3. Since one anchor element is expanded to 9 anchor elements in an expansion layer, there are 9 filters for each class (cc, ca, oc and oa). Instead of applying one filter to every RIS element of a class as output of itself, as described in Section III-C, we apply 9 filters to every anchor element as output of the same RIS element and the adjacent 8 RIS elements. The output of RIS element n using filter j is computed as

$$\mathbf{f}_{uv(n,j),i+1} = \begin{pmatrix} \text{ReLU}(\mathbf{W}_{i,j}^{cc} \mathbf{f}_{un,i} + \mathbf{b}_{i,j}^{cc}) \\ (\sum_{n'} \text{ReLU}(\mathbf{W}_{i,j}^{co} \mathbf{f}_{un',i} + \mathbf{b}_{i,j}^{co})) / N \\ (\sum_{u' \neq u} \text{ReLU}(\mathbf{W}_{i,j}^{oc} \mathbf{f}_{u'n,i} + \mathbf{b}_{i,j}^{oc})) / (U - 1) \\ (\sum_{u' \neq u} \sum_{n'} \text{ReLU}(\mathbf{W}_{i,j}^{oo} \mathbf{f}_{u'n',i} + \mathbf{b}_{i,j}^{oo})) / (N(U - 1)) \end{pmatrix}, \quad (6)$$

where $\nu(n, j)$ is the RIS element index when applying filter j for input of RIS element n . According to Figure 3 and assuming that the RIS element index begins from 1 with the upper left corner, increases first along rows and then changes to the next row (i.e., the index in row w and column h is $h + (w - 1) \cdot H$, where H is the number of columns of the RIS array.), we have

$$\nu(n, j) = \begin{cases} n - H - 2 + j & j = 1, 2, 3, \\ n - 5 + j & j = 4, 5, 6, \\ n + H - 8 + j & j = 7, 8, 9. \end{cases} \quad (7)$$

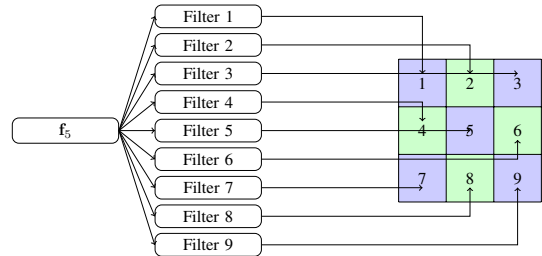
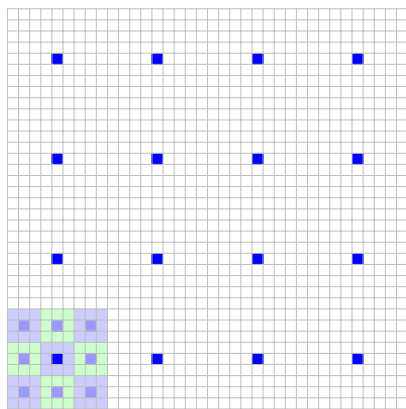


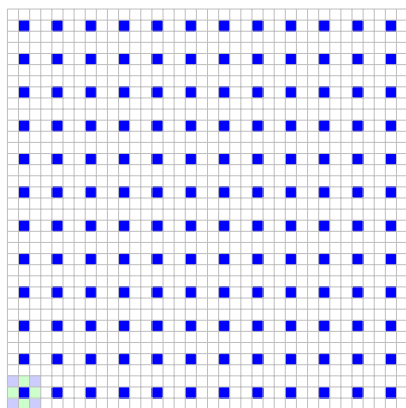
Figure 3. Application of 9 filters to expand from one anchor RIS element to 9 RIS elements, where \mathbf{f}_5 is the channel feature of RIS element 5. Indices of user and layer are omitted for simplicity since the expansion is for RIS elements.

By defining two such expansion layers, the numbers of anchor elements are increased by a factor of 9 in both row and column. If we have 16 RIS elements (4×4) with CSI, we can generate phase shifts of 1296 (36×36) RIS elements². This process is illustrated in Figure 4, where the blue RIS elements in Figure 4(a) can estimate the channel from the pilot signals from the users. Such RIS elements are only 1/81 of all RIS elements. In an RISnet of 8 layers, layer 3 and 6 are such

²Note that the factor of 9 is fixed given the expansion layer structure and the number of expansion layers. The number of total RIS elements is determined according to the performance requirement. Besides, the number of RIS elements with CSI is required to be large enough to infer the full CSI. The assumption on number of RIS elements with CSI and the RIS size is made based on the above considerations.



(a) First expansion



(b) Second expansion

Figure 4. Expansion of considered RIS elements. Blue: anchor RIS elements. Lower left corner: example of the expansion to extend the anchor RIS elements from the blue element to the adjacent elements (light blue elements in Subfigure (a) and all elements in Subfigure (b)).

expansion layers, such that the expansion layers are roughly equally placed among the 8 layers. Other layers are normal layers described in Section III-C. It is to note that we can use tensor multiplication to implement (5), (6) and use permutation matrix to sort the RIS elements in the correct order according to (7), such that we can utilize the power of parallel computing to accelerate training and testing.

During the model training, the full CSI is still required to compute the sum-rate with (3). However, phase shifts of all RIS elements Φ are computed with the partial CSI, which means that only the partial CSI is required in application.

The training process is formulated in Algorithm 1.

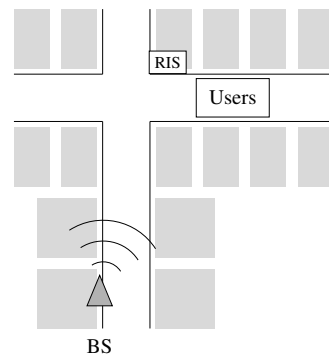


Figure 5. The ray-tracing scenario.

Algorithm 1 RISnet training

- 1: Randomly initialize RISnet.
 - 2: **repeat**
 - 3: Randomly select a batch of data samples.
 - 4: Compute precoding matrix with current RIS configuration.
 - 5: Compute $\Phi = N_{\theta}(\Gamma)$ for every data sample.
 - 6: Compute the channel \mathbf{C} for every data sample.
 - 7: Compute the objective function for every data sample.
 - 8: Compute the gradient of the objective w.r.t. the neural network parameters
 - 9: Perform a stochastic gradient ascent step
 - 10: **until** Predefined number of iterations achieved
-

IV. TRAINING AND TESTING RESULTS

We use the open-source DeepMIMO ray-tracing data set [20] to generate realistic ray-tracing channel data, where positions of BS and RIS are fixed and positions of users are uniformly distributed in the given area. We generate a training set and a testing set with different random user positions, i.e., the channel data in training set and testing set are different, and independently and identically distributed. The positions of BS, RIS and users are chosen to satisfy the following criterion: 1) There are LoS propagation paths between BS and RIS, RIS and users, but not between BS and users directly, otherwise the direct channel is so strong that the RIS does not play a significant role. 2) There are multi-path components (MPCs) between BS and RIS such that the channel matrix \mathbf{H} has a high rank because the number of served users cannot be greater than the matrix rank. 3) The minimum distance between users in a group for SDMA is 8 meters, such that the channel matrix \mathbf{G} has a high rank. Following these criteria, the designed scenario is shown in Figure 5.

We choose the Adam optimizer with a learning rate of 10^{-3} for the training. A batch with 512 data samples is randomly sampled for a training iteration. We compute the WMMSE precoding matrix \mathbf{V} with the current RIS configuration for each data sample. The gradient of (3) is computed with respect to the neural network parameter θ , which is updated with the Adam optimizer.

In the ray-tracing model, all the RIS elements share the same propagation paths (e.g., LoS path, reflection path on the ground or on a building) with different pathlosses and complex phases due to the different positions of the RIS element. The strongest path (the LoS path) is at least 1.5 times stronger than the second-strongest path. There are up to four propagation paths from the RIS to a user due to the limited number of reflectors nearby. In this case, the CSI of a few RIS elements would be representative of CSI of all RIS elements. In the opposite extreme case, if the channel comprises infinitely many and weak MPCs due to isotropic scattering, channel gains are independent and identically distributed (i.i.d.) complex Gaussian random variables in the RIS elements [21]. In this case, the full CSI cannot be inferred from the partial CSI. Between the two extreme cases, the channel gain is contributed by both deterministic strong MPCs and i.i.d. complex Gaussian gain due to weak scattering. Training and testing results using the above three channel models are shown in Figure 6.

Besides the observation that the training and testing results are very similar, which suggests there is no overfitting, an important conclusion is that the performance with partial CSI depends on the channel model. Assuming the ray-tracing channel model (i.e., there are multiple specular propagation paths, which contribute to channel gains of all RIS elements), RISnet with partial CSI achieves a similar performance to the RISnet with full CSI (Figure 6(a)). The ray-tracing channel model fulfills the requirement to apply the partial CSI. On the contrary, assuming i.i.d. complex Gaussian channel gain, the 1/81 partial CSI does not provide sufficient information about the full channel and RISnet with partial CSI does not work (Figure 6(c)). Between the two extreme cases, i.i.d. channel gains due to infinitely many and weak scattering MPCs exist but are not dominant compared to the deterministic strong propagation paths. RISnet with partial CSI has a slightly worse performance than RISnet with full CSI because the channel gain is contributed by both deterministic paths and i.i.d. scattering paths (Figure 6(b)).

The contribution of scattering paths depends mainly on the number, sizes and roughness of the scatterers as well as the frequency. The more, rougher and smaller the scatterers are in the surrounding environment, the more important scattering paths there are in the channel [22]. According to [23], scattering can be safely ignored in frequency band between 300 MHz and 3 GHz, suggesting that the proposed method would work in this frequency band.

Figure 7 shows the achieved sum-rate with three channel models and different settings, where the discrete phase shifts are 0 , $\frac{1}{2}\pi$, π and $\frac{3}{2}\pi$. Simple rounding is applied to convert continuous phase shift to discrete phase shift. We choose random phase shift and the BCD algorithm [3] as baselines. We observe that the difference between continuous and discrete phase shifts is only marginal for the resolution of $\frac{1}{2}\pi$. Sum-rate with partial CSI is comparable to sum-rate with full CSI for deterministic ray-tracing channel model and deterministic channel model plus i.i.d. perturbation. Moreover, the RISnet outperforms the two baselines considerably except RISnet with

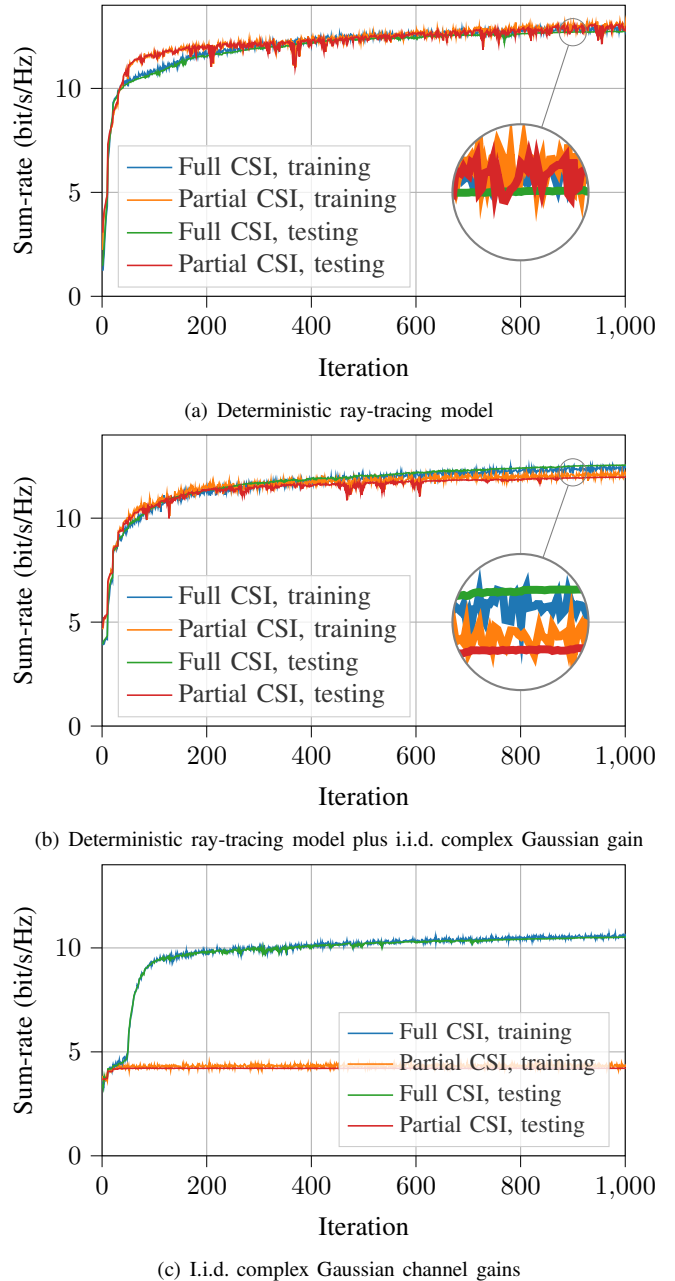


Figure 6. Training results with different spatial correlation between RIS elements.

partial CSI and i.i.d. channel models. The BCD algorithm employs full CSI but applies suboptimal approximation, which makes it more efficient but the performance is degraded. Nevertheless, it still requires more than 10 minutes to run 2000 iterations in order to compute the suboptimal RIS phase shifts for one channel realization. Compared to it, although the training of RISnet takes a long time, application of a trained RISnet to a new channel realization is done in a few milliseconds, and the performance is better than the BCD algorithm, which makes the proposed method more suitable as a high-performance, real-time solution.

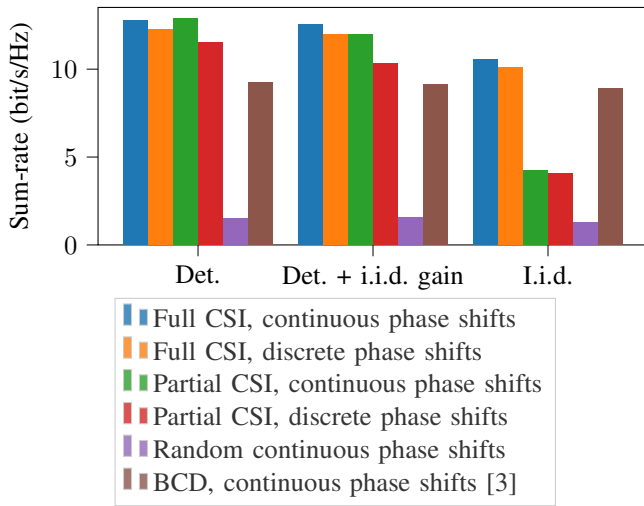


Figure 7. Test results with different spatial correlation between RIS elements and settings (Det. = deterministic ray-tracing model, I.i.d. = i.i.d. complex Gaussian channel gain).

V. CONCLUSION

The RIS is a promising technology for future wireless communications to optimize the channel property for better performance, but it faces two major challenges: scalability and the assumption of full CSI, which can be difficult to obtain in practical scenarios. In this work, we propose an NN architecture RISnet, which is scalable because its number of parameters is independent from the number of RIS elements (we assume 1296 RIS elements in the simulation) and requires CSI of a small portion of elements (16 elements in our simulation, i.e., 1/81 of all elements). The RISnet and the WMMSE precoder are applied for SDMA for a multi-antenna BS and multiple users. Simulation results show that the RISnet with full CSI outperforms two baselines for all types of channels and the RISnet with partial CSI outperforms the baselines for deterministic ray-tracing channels and ray-tracing channels plus i.i.d. complex Gaussian channel gains due to scattering. Moreover, discrete phase shifts with a granularity of $\frac{1}{2}\pi$ only cause moderate performance loss. Source code and data of this paper are available under https://github.com/bilepeng/risnet_partial_csi.

REFERENCES

- [1] M. Di Renzo, A. Zappone, M. Debbah, *et al.*, “Smart radio environments empowered by reconfigurable intelligent surfaces: How it works, state of research, and the road ahead,” *IEEE Journal on Selected Areas in Communications*, vol. 38, no. 11, pp. 2450–2525, 2020.
- [2] Q. Shi, M. Razaviyayn, Z.-Q. Luo, and C. He, “An iteratively weighted MMSE approach to distributed sum-utility maximization for a MIMO interfering broadcast channel,” *IEEE Transactions on Signal Processing*, vol. 59, no. 9, pp. 4331–4340, 2011.
- [3] H. Guo, Y.-C. Liang, J. Chen, and E. G. Larsson, “Weighted sum-rate maximization for reconfigurable intelligent surface aided wireless networks,” *IEEE Transactions on Wireless Communications*, vol. 19, no. 5, pp. 3064–3076, 2020.

- [4] C. Huang, A. Zappone, M. Debbah, and C. Yuen, “Achievable rate maximization by passive intelligent mirrors,” in *2018 IEEE International Conference on Acoustics, Speech and Signal Processing (ICASSP)*, IEEE, 2018, pp. 3714–3718.
- [5] X. Liu, C. Sun, and E. A. Jorswieck, “Two-user SINR region for reconfigurable intelligent surface aided downlink channel,” in *2021 IEEE International Conference on Communications Workshops (ICC Workshops)*, IEEE, 2021, pp. 1–6.
- [6] G. Zhou, C. Pan, H. Ren, K. Wang, and A. Nallanathan, “Intelligent reflecting surface aided multigroup multicast MISO communication systems,” *IEEE Transactions on Signal Processing*, vol. 68, pp. 3236–3251, 2020.
- [7] Z. Li, M. Hua, Q. Wang, and Q. Song, “Weighted sum-rate maximization for multi-IRS aided cooperative transmission,” *IEEE Wireless Communications Letters*, vol. 9, no. 10, pp. 1620–1624, 2020.
- [8] Q. Wu and R. Zhang, “Beamforming optimization for wireless network aided by intelligent reflecting surface with discrete phase shifts,” *IEEE Transactions on Communications*, vol. 68, no. 3, pp. 1838–1851, 2019.
- [9] R. Long, Y.-C. Liang, Y. Pei, and E. G. Larsson, “Active reconfigurable intelligent surface-aided wireless communications,” *IEEE Transactions on Wireless Communications*, vol. 20, no. 8, pp. 4962–4975, 2021.
- [10] M. A. Elmassallamy, H. Zhang, R. Sultan, *et al.*, “On Spatial Multiplexing Using Reconfigurable Intelligent Surfaces,” *IEEE Wireless Communications Letters*, vol. 10, no. 2, pp. 226–230, 2021. DOI: 10.1109/LWC.2020.3025030. arXiv: 2009.07064 [eess.SP].
- [11] M. Najafi, V. Jamali, R. Schober, and H. V. Poor, “Physics-based modeling and scalable optimization of large intelligent reflecting surfaces,” *IEEE Transactions on Communications*, vol. 69, no. 4, pp. 2673–2691, 2020.
- [12] K. Hornik, M. Stinchcombe, and H. White, “Multilayer feed-forward networks are universal approximators,” *Neural networks*, vol. 2, no. 5, pp. 359–366, 1989.
- [13] B. Sheen, J. Yang, X. Feng, and M. M. U. Chowdhury, “A deep learning based modeling of reconfigurable intelligent surface assisted wireless communications for phase shift configuration,” *IEEE Open Journal of the Communications Society*, vol. 2, pp. 262–272, 2021.
- [14] T. Jiang, H. V. Cheng, and W. Yu, “Learning to reflect and to beamform for intelligent reflecting surface with implicit channel estimation,” *IEEE Journal on Selected Areas in Communications*, vol. 39, no. 7, pp. 1931–1945, 2021.
- [15] Ö. Özdoğan and E. Björnson, “Deep learning-based phase reconfiguration for intelligent reflecting surfaces,” in *2020 54th Asilomar Conference on Signals, Systems, and Computers*, IEEE, 2020, pp. 707–711.
- [16] K. Feng, Q. Wang, X. Li, and C.-K. Wen, “Deep reinforcement learning based intelligent reflecting surface optimization for MISO communication systems,” *IEEE Wireless Communications Letters*, vol. 9, no. 5, pp. 745–749, 2020.
- [17] M. Jung and W. Saad, “Meta-learning for 6G communication networks with reconfigurable intelligent surfaces,” in *ICASSP 2021-2021 IEEE International Conference on Acoustics, Speech and Signal Processing (ICASSP)*, IEEE, 2021, pp. 8082–8086.
- [18] J. An, C. Xu, Q. Wu, *et al.*, “Codebook-based solutions for reconfigurable intelligent surfaces and their open challenges,” *IEEE Wireless Communications*, 2022.
- [19] B. Peng, F. Siegmund-Poschmann, and E. A. Jorswieck, “RISnet: A dedicated scalable neural network architecture for optimization of reconfigurable intelligent surfaces,” in *WSA & SCC 2023; 26th International ITG Workshop on Smart Antennas and 13th Conference on Systems, Communications, and Coding*, VDE, 2023, pp. 1–6.

- [20] A. Alkhateeb, "DeepMIMO: A generic deep learning dataset for millimeter wave and massive MIMO applications," in *Proc. of Information Theory and Applications Workshop (ITA)*, San Diego, CA, 2019, pp. 1–8.
- [21] V. Jamali, W. Ghanem, R. Schober, and H. V. Poor, "Impact of channel models on performance characterization of RIS-assisted wireless systems," in *European Conference on Antennas and Propagation (EuCAP)*, 2023.
- [22] S. Ju, S. H. A. Shah, M. A. Javed, *et al.*, "Scattering mechanisms and modeling for terahertz wireless communications," in *ICC 2019-2019 IEEE International Conference on Communications (ICC)*, IEEE, 2019, pp. 1–7.
- [23] T. S. Rappaport, "Wireless communications—principles and practice," *Microwave Journal*, vol. 45, no. 12, pp. 128–129, 2002.

This figure "fig1.png" is available in "png" format from:

<http://arxiv.org/ps/2305.00667v2>